The First and Second Cytoplasmic Loops of the G-Protein Receptor, Rhodopsin, Independently Form β-Turns[†]

Philip L. Yeagle,*[,‡] James L. Alderfer,[§] Alexender C. Salloum,[‡] Laith Ali,[‡] and Arlene D. Albert[‡]

Department of Biochemistry, School of Medicine and Biomedical Sciences, State University of New York at Buffalo, Buffalo, New York 14214, and Department of Biophysics, Roswell Park Cancer Institute, Buffalo, New York 14263

Received September 23, 1996; Revised Manuscript Received January 2, 1997[⊗]

ABSTRACT: The cytoplasmic face of the transmembrane protein, rhodopsin, is made up of one carboxyl terminal and three cytoplasmic loops connecting six of the seven transmembrane helices. Neither the high-resolution, three-dimensional structure of this G-protein receptor nor any other cell surface receptor is known. In this work, the structures of peptides containing the amino acid sequence of the first and second cytoplasmic loops of rhodopsin have been determined. Both loops show ordered structures in solution. In both loops, the ends of the transmembrane helices unwind and form a β-turn. The conformations of the two loops are remarkably similar, even though their sequences are not. These data suggest a structural motif for short loops in transmembrane proteins. The well-ordered structures of these loops, in the absence of the transmembrane helices, indicate that the primary sequences of these loops stabilize the β-turn. These data further suggest that the loops may contribute to the folding of such membrane proteins during their synthesis and insertion into membranes.

Integral membrane proteins contain hydrophobic, transmembrane domains and extramembraneous domains that contact the aqueous phase. The roles of these domains in membrane protein structure and stability have been the subject of study (Kahn et al., 1992). However, crucial structural information on transmembrane proteins has been lacking.

Membrane proteins must be inserted into a bilayer during synthesis. For membrane proteins that traverse the membrane more than once in the form of α-helices, loops must form to connect the transmembrane helices. The hydrophobic effect and the packing of the helices could be the dominant driving force which determines the folding of these loops and their insertion into the membrane. Alternatively, the loops could have an independent, well-defined structure which could then define a helical hairpin and lead to an insertion of a largely prefolded section of the protein into the membrane during synthesis. A hypothesis for insertion of secreted and membrane proteins was described (Engelman & Steitz, 1981). This hypothesis emphasized the role of helix−helix interactions in the formation of a helical dimer with a connecting loop preparatory to insertion of the helical hairpin structure in the membrane. Such a folding pattern was proposed as part of the pathway for folding and insertion of a transmembrane protein or as part of the secretory process.

The role of the connecting loop deserves additional attention. Previous work on the linkage region of a signal sequence of a secreted protein suggested that the linkage region is a β-turn (Duffaud & Inouye, 1988). Recent work on the insertion of transmembrane helices of integral membrane proteins suggested that the connecting peptide must form a loop and that the loop will stabilize the formation of a dimer of transmembrane helices in preparation for membrane insertion (Lin & Addison, 1995). However, no information is presently available on whether the connecting loops of a transmembrane protein have, within the primary sequence, the information necessary to form a defined turn in the absence of the hydrophobic transmembrane helices.

Recent results have revealed that the extramembraneous portions of rhodopsin, a G-protein receptor, act structurally and biologically as protein domains. The carboxyl terminal domain and the third cytoplasmic loop both have biological activity, inhibiting the activation of the G protein, transducin, by light-activated rhodopsin (Takemoto et al., 1986; Konig et al., 1989). Both these protein domains form compact globular structures in solution as determined by multidimensional nuclear magnetic resonance (NMR)[1] (Yeagle et al. 1995a,b). These successful structures offer support for an alternate approach to membrane protein structure, in which the extramembraneous domains of the integral membrane protein can be solved, using standard techniques, and the resulting structures docked with the helices of the transmembrane domain (Schertler et al., 1993; Unger & Schertler, 1995).

In this study, the structures of the first and second cytoplasmic loops (see Figure 1) are investigated as free peptides. Of these two, the latter exhibits biological activity in solution, inhibiting the activation of G protein, transducin, by light-activated rhodopsin (Konig et al., 1989). As in the case of the carboxyl terminal domain and the third cytoplasmic loop, biological activity is a useful indicator of whether the structure in solution retains important structural elements of the activated receptor. These loops contain a

[†] This work was supported by National Institutes of Health Grant EY03328 and in part by Grant CA16056.

* Corresponding author.
[‡] State University of New York at Buffalo.
[§] Roswell Park Cancer Institute.

[⊗] Abstract published in *Advance ACS Abstracts,* March 15, 1997.

[1] Abbreviations: HPLC, high-pressure liquid chromatography; NMR, nuclear magnetic resonance; NOE, nuclear Overhauser effect; rhoI, the first cytoplasmic loop of rhodopsin; rhoII, the second cytoplasmic loop of rhodopsin; rhoIII, the third cytoplasmic loop of rhodopsin.

S0006-2960(96)02403-8 CCC: $14.00

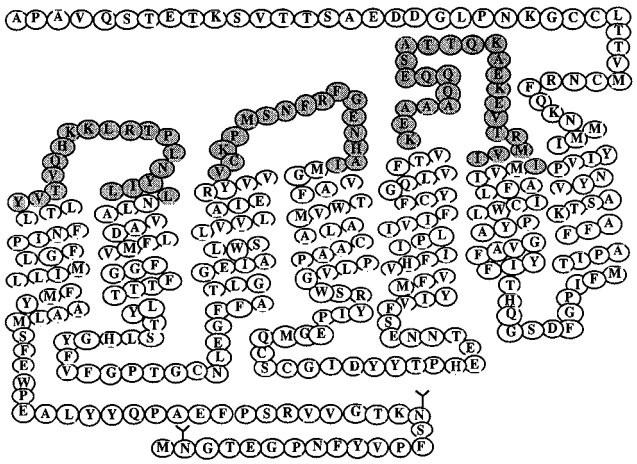

FIGURE 1: Representation of the primary sequence of bovine rhodopsin, after Hargrave (1983). The shaded portions are incorporated into rhoI, rhoII, and rhoIII.

β-turn and are compared to the third cytoplasmic loop which also forms a turn in the absence of the hydrophobic transmembrane helices. Furthermore, the amino and carboxyl termini of the peptides are separated by a distance consistent with the center to center distance of two close-packed α-helices, separate from any influence of the transmembrane helices of rhodopsin. Therefore, loops connecting hydrophobic helices of transmembrane proteins could be a determinant of integral membrane protein folding.

MATERIALS AND METHODS

Peptide Synthesis. A peptide containing the 17-amino acid sequence of the first cytoplasmic loop of bovine rhodopsin, rhoI, was synthesized through solid phase synthesis and purified by HPLC. A peptide constituting the 16 amino acid residues of the second cytoplasmic loop of bovine rhodopsin, rhoII, was synthesized in the Biopolymer Facility of the Roswell Park Cancer Institute and purified by HPLC. A peptide constituting the 26 amino acid residues of the third cytoplasmic loop of bovine rhodopsin, rhoIII, was synthesized in the Biopolymer Facility of the Roswell Park Cancer Institute and purified by HPLC. Figure 1 shows the sequences (Hargrave et al., 1983).

NMR Spectroscopy. All NMR spectra were recorded on a Bruker AMX-600 spectrometer at 10 °C in 1 mM phosphate buffer at pH 5.9, and including 0.1 mM β-mercaptoethanol for rhoII. Structures were solved at peptide concentrations of 2.5 mM. Standard pulse sequences and phase cycling were employed to record in H_2O (10% D_2O) double-quantum filtered (DQF) COSY, HOHAHA (Braunschweiler & Ernst, 1983; Bax & Davis, 1985), and NOESY (400 ms mixing time) (Kumar et al., 1980) spectra. All spectra were accumulated in a phase sensitive manner using time-proportional phase incrementation for quadrature detection in F_1. Chemical shifts were referenced to internal methanol. Sequence-specific assignments were obtained using standard approaches, and the results are listed in Tables 1−3.

Structure Refinement. The sequence-specific assignment of the ^{1}H NMR spectrum was carried out using standard methods. The overall structure of each of the peptides was determined exclusively through the use of the intraresidue and sequential NOEs. The long range NOEs were used in the refinement of the structure. Thus, the overall shapes of the loops were determined without the long range NOEs. There was no evidence for intermolecular NOEs in these experiments (i.e., long range NOEs inconsistent with the overall structure determined as described above). Assigned

Table 1: ^{1}H Chemical Shifts for rhoI

residue	αH	NH	βH	other	
Tyr1	4.27		3.1	7.11	6.86
Val2	4.21	8.515	2.0	0.92	
Thr3	4.32	8.505	4.14	1.21	
Val4	4.04	8.455	2.0	0.92, 0.84	
Gln5	4.29	8.61	1.91, 2.0	2.33	6.975, 7.62
His6	4.71	8.775	3.15, 3.25	7.31	
Lys7	4.30	8.58	1.74, 1.80	1.43	3.0
Lys8	4.36	8.485	1.56, 1.63	1.47	3.0
Leu9	4.34	8.545	1.8	0.88	
Arg10	4.41	8.61	1.76, 1.84	1.66, 1.60	3.2
Thr11	4.59	8.4	4.17	1.24	
Pro12	4.59		1.98, 2.32	2.02, 1.90	3.67, 3.87
Leu13	4.245	8.4	1.64, 1.56	0.88, 0.93	
Asn14	4.66	8.405	2.76	6.95, 7.68	
Tyr15	4.57	8.06	2.94, 3.00	6.815, 7.10	
Ile16	4.11	8.11	1.8	1.12, 1.44	0.84
Leu17	4.30	8.37	1.65	0.89	

Table 2: ^{1}H Chemical Shifts for rhoII

residue	αH	NH	βH	other	
Val1					
Cys2	4.565	8.87	2.92		
Lys3	4.60	8.725	1.75, 1.83	1.5	3
Pro4	4.42		2.02, 2.3	3.65, 3.87	1.9
Met5	4.48	8.66	1.91, 2.10	2.04, 2.3	
Ser6	4.40	8.46	3.78, 3.83		
Asn7	4.686	8.545	2.70, 2.75	6.92, 7.62	
Phe8	4.545	8.24	3.0	7.17, 7.27	
Arg9	4.22	8.145	1.57, 1.64	1.4	3.1
Phe10	4.505	8.30	3.05, 3.15	7.28, 7.37	
Gly11	3.79, 3.94	8.43			
Glu12	4.315	8.175	1.93, 2.05	2.39	
Asn13	4.62	8.58	2.72, 2.78	6.99, 7.67	
His14	4.645	8.46	3.14, 3.26		
Ala15	4.35	8.445	1.39		
Ile16	4.21	8.20	1.91	1.38	

Table 3: ^{1}H Chemical Shifts for rhoIII

residue	αH	NH	βH	other	
Lys1		4.036	1.75, 1.87	1.47	1.71, 3.02
Glu2	8.915	4.40	2.0, 2.09	2.50	
Ala3	8.73	4.29	1.42		
Ala4	8.50	4.27	1.41		
Ala5	8.48	4.285	1.40		
Gln6	8.44	4.30	2.01, 2.10	2.39	
Gln7	8.55	4.305	2.01, 2.12	2.40	
Gln8	8.48	4.325	2.02, 2.11	2.40	
Glu9	8.60	4.41	2.0, 2.09	2.50	
Ser10	8.60	4.45	3.91, 3.95		
Ala11	8.595	4.395	1.46		
Thr12	8.27	4.357	4.275	1.24	
Thr13	8.165	4.305	4.25	1.23	
Gln14	8.62	4.33	2.01, 2.13	2.39	
Lys15	8.41	4.25	1.78, 1.83	1.41	1.70, 3.02
Ala16	8.36	4.30	1.41		
Glu17	8.39	4.33	2.01, 2.12	2.41	
Lys18	8.40	4.29	1.76, 1.83	1.44	1.71, 3.02
Glu19	8.45	4.41	2.01, 2.12	2.48	
Val20	8.40	4.18	2.10	0.96	
Thr21	8.39	4.34	4.16	1.22	
Arg22	8.52	4.36	1.85, 1.77	1.60, 1.66	3.21, 7.26
Met23	8.54	4.49	2.03	2.53, 2.59	
Val24	8.39	4.095	2.02	0.90, 0.95	
Ile25	8.485	4.22	1.86	1.22, 1.5	0.90
Ile26	8.41	4.23	1.91	1.19, 1.47	0.91, 0.86

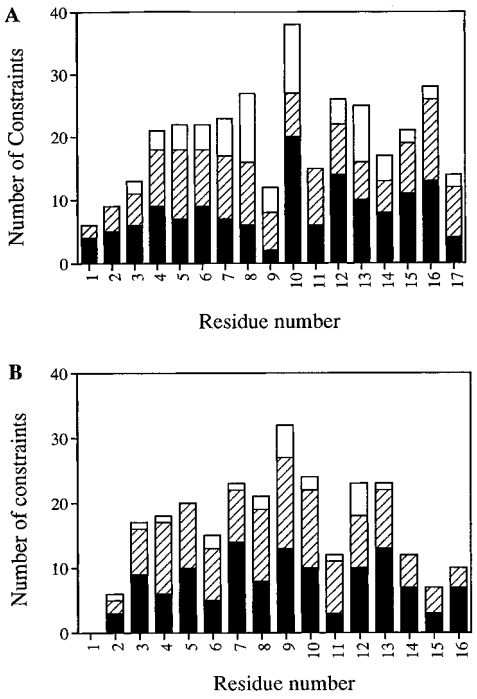

FIGURE 2: Number of constraints per residue for (A) rhoI and (B) rhoII: (filled bars) intraresidue, (hatched bars) sequential, and (open bars) long range.

NOE cross-peaks were segmented using a statistical segmentation function and characterized as strong, medium, and weak, corresponding to upper bound distance range constraints of 2.7, 3.5, and 5.0 Å, respectively. Lower bounds between nonbonded atoms were set to the sum of their van der Waals radii (approximately 1.8 Å). Pseudoatom corrections were added to interproton distance restraints where necessary (Wüthrich et al., 1983). Distance geometry calculations were carried out using the program DIANA (Guntert et al., 1991) within the SYBYL 6.2 package (Tripos Software Inc., St. Louis). First-generation DIANA structures, 150 in total, were optimized with the inclusion of three REDAC cycles. In the structures shown in the figures, all the NOE constraints were satisfied. Energy refinement calculations (restrained minimizations/dynamics) were carried out on the best distance geometry structures using the SYBYL program implementing the Kollman all-atom force field. Statistics on structures were obtained from X-plor. These calculations were performed on a Silicon Graphics 4D/440 computer. Imaging and overlaying of the resulting structures were performed on a Power Mac with MacImdad (Molecular Applications Group, Palo Alto, CA).

RESULTS AND DISCUSSION

First Cytoplasmic Loop of Bovine Rhodopsin. A 17mer containing the sequence of the first cytoplasmic loop of bovine rhodopsin (rhoI) was synthesized and its solution structure determined by standard homonuclear two-dimensional NMR protocols, as described in Materials and Methods. The sequence used can be seen in Figure 1. From the NOESY map, 240 constraints were obtained: 141 intraresidue, 65 sequential, and 34 long range. Figure 2A shows the number of constraints per residue. Table 1 lists the ^{1}H chemical shifts for rhoI.

The structure of the first cytoplasmic loop appears in Figure 4A as an overlay of the six best structures obtained from DIANA, after energy minimization. Only one set of peaks was observed for each amino acid. Only one family of structures was obtained from the DIANA calculations. There was no evidence for alternate conformations of this loop, consistent with either a single conformation or a dominant conformation that is rapidly interconverting with other minor structures.

The $C_\alpha-H$ ^{1}H chemical shifts are sensitive to conformation (Wishart et al., 1992). Using these chemical shifts, the effects of temperature, ionic strength, and concentration on the peptide conformation of rhoI were explored. An increase in ionic strength to 50 mM NaCl and a 5-fold reduction in peptide concentration had no effect on the $C_\alpha-H$ chemical shifts of rhoI. The temperature was varied between 10 and 50 °C. No evidence for denaturation was observed. These data suggest that the first cytoplasmic loop is somewhat more stable than the other two structures described below.

Second Cytoplasmic Loop of Bovine Rhodopsin. A 16mer containing the sequence of the second cytoplasmic loop (rhoII) was synthesized. The sequence used can be seen in Figure 1. Preliminary differential scanning calorimetry experiments revealed a thermal transition for this peptide at about 44 °C (A. D. Albert and R. Epand, unpublished results). Circular dichroism experiments showed the presence of modest secondary structure (data not shown). Both the calorimetry and the CD data indicated that rhoII had structure in solution. Therefore, the solution structure was determined by homonuclear two-dimensional NMR as described in Materials and Methods. NOESY data in 90% H_2O/10% D_2O were assigned and used to generate 193 constraints: 121 intraresidue, 60 sequential, and 11 long range. A portion of the NOESY map appears in Figure 4. Figure 2B shows the number of constraints per residue. Table 2 lists the ^{1}H chemical shifts for rhoII.

The structure of the second cytoplasmic loop of rhodopsin appears in Figure 3B as an overlay of the six best structures obtained with the constraints from the NOESY map, after energy minimization. Only one set of peaks was observed for each amino acid. Only one family of structures was obtained from the DIANA calculations. There was no evidence of alternate conformations of this loop.

Using the $C_\alpha-H$ ^{1}H chemical shifts, the effects of ionic strength, pH, and concentration on the peptide conformation of rhoII were explored. An increase in ionic strength to 50 mM NaCl and a change in pH from 5.9 to 7.5 had no effect on the $C_\alpha-H$ chemical shifts of rhoII. A 5-fold reduction in concentration, to 0.5 mM, resulted in a change in the $C_\alpha-H$ chemical shifts of residues 8−10, which may suggest a small concentration-dependent influence on the peptide conformation. No other changes were observed.

Third Cytoplasmic Loop of Rhodopsin. A structure was previously published for a 22-amino acid peptide representing the third cytoplasmic loop of rhodopsin (Yeagle et al., 1995b). Structure was defined for only the middle third of that peptide, due to a lack of sufficient constraints. More recently, the peptide was extended by the addition of four amino acids on the carboxyl terminal of the peptide. Table 3 shows the chemical shifts. This longer peptide exhibited a modest increase in ordering compared to the shorter peptide studied previously, and additional constraints. A total of 277 constraints were used: 158 intraresidue, 70 sequential, and 49 long range. Figure 5 shows the number of constraints per residue. Figure 6A shows an overlay of the six best

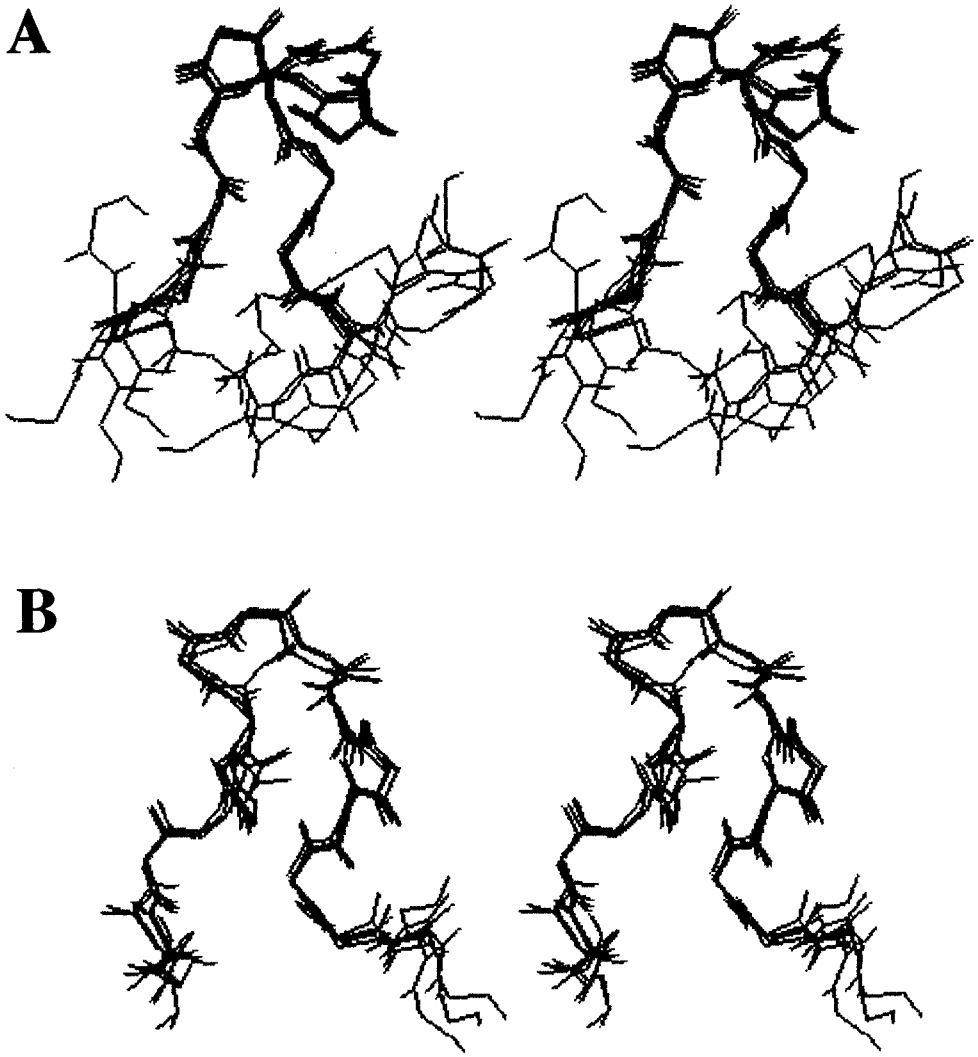

FIGURE 3: Stereoview of the overlay of the six best structures obtained for rhoI and rhoII: (A) rhoI, rmsd for main chain atoms (residues 2−14) = 0.97 Å; and (B) rhoII, rmsd for main chain atoms (residues 1−14) = 0.51 Å.

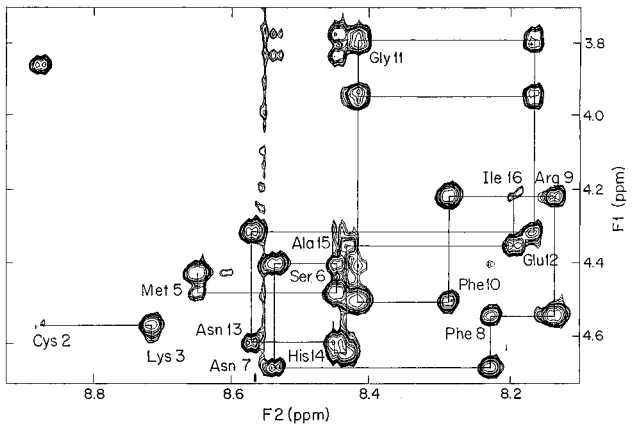

FIGURE 4: Portion of the NOESY map for the second cytoplasmic loop of rhodopsin with assignments labeled. The numbering is internal within the peptide. Cys2 corresponds to Cys140 in the whole rhodopsin structure.

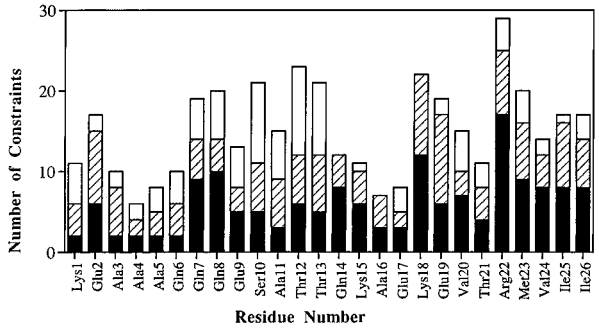

FIGURE 5: Number of constraints per residue for rhoIII: (filled bars) intraresidue, (hatched bars) sequential, (and (open bars) long range.

structures from a DIANA run, obtained as described above, and Figure 6B shows a representative structure in stereo. Although this structure determination still suffers from a lack of adequate constraints (due in part to coincidence of key peaks in the NOESY map), the outline of the loop can be seen.

The structure in Figure 3A of the first cytoplasmic loop of rhodopsin exhibits several remarkable features. One is that most of the structure is reasonably well-ordered, even though it is relatively small. Second, the structure forms a β-turn. There are hydrogen bonds across this turn between the NH of Leu9 and the C═O of His6 and between the NH of Arg10 and the C═O of Gln5. Third, the amino terminal and the carboxyl terminal of the peptides are located close to each other, thus completing the loop and positioning these termini appropriately for connection with adjacent trans-

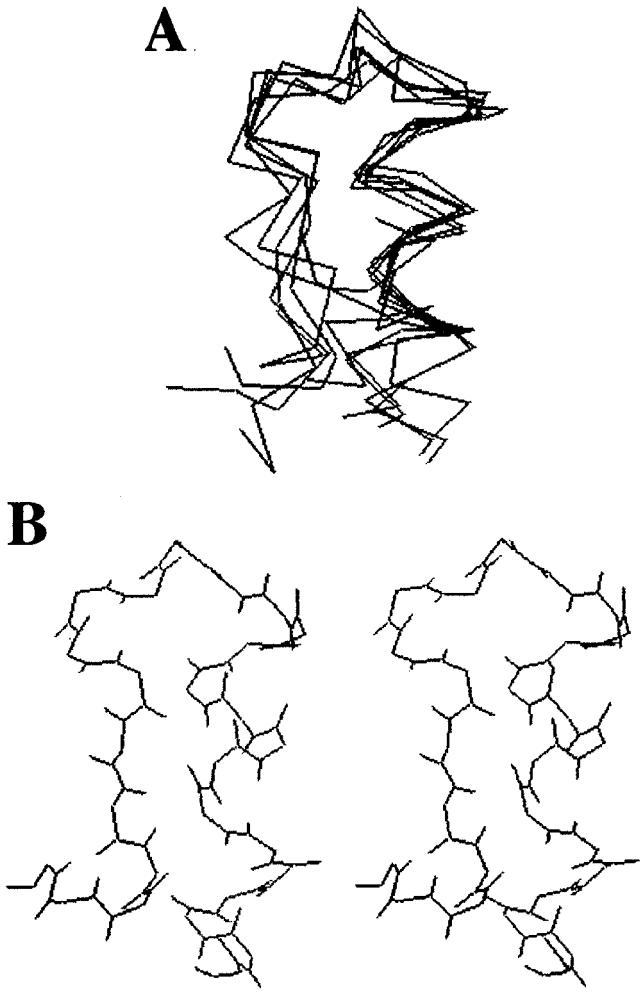

FIGURE 6: Structure of the third cytoplasmic loop of rhodopsin. This is a further refinement of a structure reported previously (Yeagle et al., 1995b), with the addition of four residues on the carboxyl terminal end of the peptide. (A) Overlay of the six best DIANA structures using just the α-carbons. (B) One of the structures from part A in stereo, showing all the backbone atoms.

membrane helices as would be expected to occur in the intact rhodopsin.

Neither side of this turn shows α-helical structure. The peptide includes the entire hydrophilic region of this cytoplasmic domain. Therefore, putative transmembrane helices 1 and 2 of rhodopsin apparently do not extend beyond the hydrophobic transmembrane region on the cytoplasmic face.

Remarkably, the structure of the second cytoplasmic loop also reveals a β-turn in the middle of the peptide (Figure 3B), most closely related to type I (Sibanda et al., 1989). Across this β-turn, a hydrogen bond is formed between the NH of Arg9 and the C═O of Ser6. Both the amino terminal end and the carboxyl terminal end form structures that are helical. These helical ends are likely continuations of the transmembrane α-helices of rhodopsin which are connected by this β-turn. These helical regions are not α-helices but adopt a more open structure. The observed structure is consistent with an unwinding of both of the transmembrane helices as they enter the second cytoplasmic loop and make the turn. This observation is consistent with the site-directed spin labeling of this loop of rhodopsin, in which it was concluded that transmembrane helix 3 extends to Cys140 (Cys2 in this structure), but likely not beyond (Farahbakhsh et al., 1995). As in the case of the first cytoplasmic loop, the structure of the second cytoplasmic loop shows the amino and carboxyl termini close to each other, appropriate for connection to their respective, adjacent, transmembrane helices.

FIGURE 7: Superposition of the average structures of the first and the second cytoplasmic loops of rhodopsin.

FIGURE 8: Superposition of the second cytoplasmic loop of rhodopsin (rhoII) and the loop from bacteriorhodopsin containing residues 55−70 (2BRD).

The structures of the first and second cytoplasmic loops can be compared. Figure 7 shows a superposition of the two loops. The structures of the two loops are similar. Thus, the primary sequences of both the first and the second cytoplasmic loops of this integral membrane protein contain the information content to make the requisite turn, without the influence of the transmembrane helices to which the turns are connected. The similarity of their structure suggests that these structures may represent a motif for short loops of transmembrane proteins. Interestingly, one loop of a recently reported structure for bacteriorhodopsin (Grigorieff et al., 1996) shows a structure similar to the loops reported here, as seen in the overlay in Figure 8.

Furthermore, these results suggest that during biosynthesis the first and second cytoplasmic loops can each form a turn and thus stabilize the formation of a helical hairpin for insertion into the membrane. Previous calorimetric results suggested that the turns of bacteriorhodopsin (Gilles-Gonzalez et al., 1991) and rhodopsin (Kahn et al., 1992) may contribute to the stability of the respective protein. Therefore, in the helical hairpin hypothesis (Engelman & Steitz, 1981), both the turn and the helix−helix interactions may be important.

The third cytoplasmic loop offers a different motif. Recent spin labeling experiments have suggested that the 227−231 region represents the interfacial region between the hydrophobic portion of helix 5 and the third cytoplasmic loop (Altenbach et al., 1996). This region is at the amino terminal of rhoIII. The structure of rhoIII, therefore, is consistent with an extension of helix 5 well above the membrane surface on the cytoplasmic face. That conclusion is consistent with the periodicity observed in the aforementioned spin labeling experiments. At the top of this helix, the structure im-

mediately enters the turn and returns to the membrane interface. There are insufficient constraints on the carboxyl terminal portion of this peptide to determine whether that portion is also an α-helix, as has been suggested (Altenbach et al., 1996), or is a more open helical structure as found in rhoI and rhoII. In another structure determination, we have recently found that the carboxyl terminal of rhodopsin contains an extension of helix 7 (Yeagle et al., 1996). Therefore, at least two of the transmembrane helices of rhodopsin extend beyond the hydrophobic region on the cytoplasmic face of the protein.

ACKNOWLEDGMENT

We thank Dr. R. Wollman for computational assistance and J. Young for technical assistance.

REFERENCES

Altenbach, C., Yang, K., Farrens, D. L., Farahbakhsh, Z. T., Khorana, H. G., & Hubbell, W. L. (1996) *Biochemistry 35*, 12470−12478.
Bax, A., & Davis, D. G. (1985) *J. Magn. Reson. 65*, 355.
Braunschweiler, L., & Ernst, R. R. (1983) *J. Magn. Reson. 53*, 521.
Duffaud, G., & Inouye, M. (1988) *J. Biol. Chem. 263*, 10224−10228.
Engelman, D. M., & Steitz, T. A. (1981) *Cell 23*, 411−422.
Farahbakhsh, Z. T., Ridge, K. D., Khorana, H. G., & Hubbell, W. L. (1995) *Biochemistry 34*, 8812−8819.
Gilles-Gonzalez, M. A., Engelman, D. M., & Khorana, H. G. (1991) *J. Biol. Chem. 266*, 8545−8550.
Grigorieff, N., Ceska, T. A., Downing, K. H., Baldwin, J. M., & Henderson, R. (1996) *J. Mol. Biol. 259*, 393−421.
Guntert, P., Braunk, W., & Wuthrich, K. (1991) *Mol. Biol. 217*, 517−530.
Hargrave, P. A., McDowell, J. H., Curtis, D. R., Wang, J. K., Juszczak, E., Fong, S. L., Rao, J. K. M., & Argos, P. (1983) *Biophys. Struct. Mech. 9*, 235−244.
Kahn, T. W., Sturtevant, J. M., & Engelman, D. M. (1992) *Biochemistry 31*, 8829−8839.
Konig, B., Arendt, A., McDowell, J. H., Kahlert, M., Hargrave, P. A., & Hofmann, K. P. (1989) *Proc. Natl. Acad. Sci. U.S.A. 86*, 6878−6882.
Kumar, A., Ernst, R. R., & Wuthrich, K. (1980) *Biochem. Biophys. Res. Commun. 95*, 1−6.
Lin, J., & Addison, R. (1995) *J. Biol. Chem. 270*, 6935−6941.
Schertler, G. R. X., Villa, C., & Henderson, R. (1993) *Nature 362*, 770−772.
Sibanda, B. L., Blundell, T. L., & Thornton, J. M. (1989) *J. Mol. Biol. 206*, 759−777.
Takemoto, D. J., Morrison, D., Davis, L. C., & Takemoto, L. J. (1986) *Biochem. J. 235*, 309−312.
Unger, V. M., & Schertler, G. F. X. (1995) *Biophys. J. 68*, 1776−1786.
Wishart, D. S., Sykes, B. D., & Richards, F. M. (1992) *Biochemistry 31*, 1647−1651.
Wüthrich, K., Billeter, M., & Braun, W. J. (1983) *J. Mol. Biol. 169*, 949−961.
Yeagle, P. L., Alderfer, J. L., & Albert, A. D. (1995a) *Nat. Struct. Biol. 2*, 832−834.
Yeagle, P. L., Alderfer, J. L., & Albert, A. D. (1995b) *Biochemistry 34*, 14621−14625.
Yeagle, P. L., Alderfer, J. L., & Albert, A. D. (1996) *Mol. Vision 2* (http://www.emory.edu/molvis/v2/yeagle).

BI962403A